JOURNAL OF CATALYSIS 135, 269–286 (1992)

Reduction and Metathesis Activity of MoO_3/Al_2O_3 Catalysts

I. An XPS Investigation of MoO_3/Al_2O_3 Catalysts

WOLFGANG GRÜNERT,* ALEKSANDER YU. STAKHEEV,† WOLFGANG MÖRKE,‡ REINHARD FELDHAUS,* KLAUS ANDERS,* EFIM S. SHPIRO,† AND KHABIB M. MINACHEV†

*Central Institute of Organic Chemistry, Permoserstrasse 15, Leipzig, O-7050, Germany; †USSR Academy of Sciences, N. D. Zelinsky Institute of Organic Chemistry, 117913 Moscow, Leninsky Prospect 47, USSR; and ‡Technical University Merseburg, Otto-Nuschke-Strasse, Merseburg, O-4200, Germany

Received November 6, 1990; revised December 12, 1991

MoO_3/Al_2O_3 catalysts (2–13 wt% MoO_3) were investigated by XPS in the oxidized form, after thermal treatment in flowing Ar (973 K), and after reduction in H_2 (673–973 K), which are conditions typically employed in the activation of these catalysts for the metathesis reaction. A new assignment of Mo 3*d* binding energies to Mo oxidation states was applied in the analysis of the reduced samples. During the thermal treatment in flowing Ar, part of the hexavalent Mo present in the initial samples underwent reduction to Mo(V), which could also be detected by EPR. The reduction of alumina-supported Mo(VI) in H_2 was found to produce surfaces, on which Mo(VI), Mo(V), Mo(IV), Mo(II), and, at reduction temperatures above 900 K, Mo(0), coexist. For reduction temperatures of about 800 K, distributions of these Mo states, which differ from those reported in the literature by a Mo(V) contribution not exceeding 10% of the total Mo and by the presence of Mo(II), were derived. When reduced MoO_3/Al_2O_3 catalysts were subsequently treated in flowing inert gas at 973 K a partial reoxidation of the surface was observed. © 1992 Academic Press, Inc.

INTRODUCTION

Among the numerous reactions catalyzed by molybdenum, the metathesis reaction attracts particular interest as it provides a close relation between heterogeneous and homogeneous catalysis. The mechanism of the homogeneously catalyzed metathesis was shown to involve metal carbene complexes (*1–3*). It is widely accepted that analoguous surface carbene species are formed from oxidic precursors on the surface of heterogeneous metathesis catalysts (*4–8*). In accordance with numerous reports on the beneficial effect of reductive catalyst pretreatments on the metathesis activity (*7, 9–11*), it has been shown with model catalytic systems that the carbene sites originate from species containing Mo in the +4 oxidation state (*5, 12, 13*).

Nevertheless, open questions remain. On one hand, these concern preparations involving Mo carbonyl compounds, where the assignment of the metathesis activity to Mo species of low oxidation state (+2, +3 (*14*), on Al_2O_3) has been reaffirmed quite recently (0 (*15*), on Y zeolite support). On the other hand, some metathesis activity is frequently found with unreduced oxide catalysts (*7, 10, 11*), which were found to be activated by a reaction with the olefin at a temperature as low as room temperature (*6, 16*). This may suggest the presence of a second active site precursor with higher valency. Indeed, highly active homogeneous metathesis catalysts often involve Mo or W in high oxidation states, e.g., Mo(VI) and W(VI) (*17, 18*). The hexavalent state, however, is rarely considered as a candidate for an active site precursor in heterogeneous catalysts as the pronounced break-in phenomena observed with silica-supported W and Mo catalysts (*19*) imply its irrelevance to the metathesis reaction. A suggestion of

0021-9517/92 $3.00
Copyright © 1992 by Academic Press, Inc.
All rights of reproduction in any form reserved.

active site precursors involving Mo(VI) made in (*16*) was later qualified by the same authors by the statement that a slight reduction of the surface as indicated by the emergence of a Mo(V) EPR signal is also essential for the activation (*6*). Convincing evidence for the role of hexavalent Mo species as active site precursors has been reported for photocatalytic metathesis processes (*7, 20*).

In our former XPS and catalytic investigations of WO_3/Al_2O_3 metathesis catalysts we found that active sites may be derived from tungsten species of both +6 and +4 oxidation states, the former being responsible for the reactivity of thermally activated samples (*21, 22*). In the same project, $W(V)/Al_2O_3$ was excluded as an active site precursor by EPR measurements (*23*). In the present study, which started from the observation of analogies in the thermal activation properties between alumina-supported MoO_3 and WO_3 (*24*), the question is raised as to whether the coexistence of hexavalent and tetravalent active site precursors may be proved also for MoO_3/Al_2O_3 catalysts. In the first part, the behavior of MoO_3/Al_2O_3 during thermal treatment in inert and reductive atmosphere is discussed on the basis of an XPS investigation complemented by some EPR measurements. The subsequent part (*25*) contains the data on metathesis activities obtained after similar catalyst treatments, from which conclusions will be drawn concerning the electronic state of Mo in the active site precursors.

After more than 15 years of effort in characterizing reduced MoO_3/Al_2O_3 surfaces by XPS (e.g., (*26–31*)), one might not expect that more relevant information could be attained from further studies in this subject. However, in the course of our work, we came to the conclusion that the widely accepted basis for the assignment of the binding energies (B.E.) of Mo 3*d* XPS lines to the Mo oxidation states in supported molybdena catalysts must be revised. We suggested an approach based on a linear relationship between the Mo B.E. and the oxidation state, as proposed first by Haber *et al.* (*32*). This approach, a substantiation of which is given in (*33*), leads to a reinterpretation of a part of the evidence obtained by XPS. The consequences are discussed in the following.

EXPERIMENTAL

1. Materials. The catalysts were prepared by impregnation of γ-Al_2O_3 (Leuna-Werke, Leuna, Germany; BET surface area $\simeq 260\ m^2\ g^{-1}$) with solutions of MoO_3 in NH_4OH (pH $\simeq$ 8) by the incipient wetness technique. After drying at 400 K, they were calcined in air at 823 K for 2 h and stored in air prior to use. In Table 1, BET surface areas, MoO_3 contents, and the resulting Mo loadings of the catalysts are summarized and the code used to denote the samples is illustrated. In all cases the MoO_3 content is well below the monolayer capacity of the alumina support, which is $\simeq$20 wt%.

H_2 and Ar from cylinders were deoxygenated over MnO/Al_2O_3, dried over a 4A molecular sieve, and repurified at the entrance of the XPS sample pretreatment system by a trap containing both MnO/Al_2O_3 and a molecular sieve. When the Ar was analyzed with the residual gas analyzer of the spectrometer employed (vide infra) no oxygen could be detected.

In a preliminary set of experiments performed on an AEI ES 200B spectrometer and with an older version of our sample transfer equipment (*34*), the carrier gases were less pure and an influence of the residual oxygen on the reduction degree was found. These experiments, which supplied only qualitative results due to lack of analyses of the residual oxygen content, will be referred to as "preliminary runs."

2. XPS measurements. For the XPS investigation, a Kratos XSAM 800 spectrometer (Mg$K\alpha$ excitation, 12 kV, 20 mA, FRR analyzer mode, pressure during data acquisition $\simeq 10^{-8}$ Torr) was used with a sample transfer system, which will be described in more detail elsewhere. This sample transfer

TABLE 1

MoO_3 Contents and BET Areas of the Catalysts

Code	MoO_3 content		BET area (calcination at 823 K)		Mo loading[b] (atoms/nm^2)	BET area after calcination[c] at	
	Nominal (wt%)	Real[a] (wt%)	$m^2\ g^{-1}$	$m^2\ g^{-1}\ Al_2O_3$		T_c (K)	($m^2\ g^{-1}$)
Mo0.5	0.5	0.45	242	243	0.08	1143	159
Mo1	1	1.1	258	261	0.18	1093	171
Mo2	2	1.8	246	251	0.31	1093	150
Mo4	4	4.5	249	261	0.76	973	234
Mo7	7	7.4	257	277	1.24	973	247
Mo13	13	12.9	234	269	2.31	973	228

[a] Determined by electron microprobe analysis.
[b] Referred to BET area after calcination at 823 K.
[c] After calcination in air for 2 h at T_c (by analogy with activation procedures used in part II (*25*), which were conducted in Ar).

system allows samples mounted on a sample holder to be treated at high temperatures and with various gaseous media without subjecting the surface of the sampling probe to the conditions of treatment. After cooling, the sample transfer system is connected to the spectrometer and the sample is transferred to the insertion lock of the latter. After the measurement, the sample can be returned to the reaction tube and a subsequent step of pretreatment can be performed. The samples were made by pressing powdered catalyst into steel gauzes. Sample heating and cooling steps as well as sample transfer were performed in flowing Ar. The conditions of sample treatment are given with the results.

The binding energies reported in this paper are referenced to Al 2*s* = 119.8 eV. With this calibration, Al 2*p* was 74.9–75.1 eV while C 1*s* was found to be in the range of 284.8–285.1 eV. The binding energies are given with an accuracy of ±0.1 eV.

The Mo 3d signal shapes were analyzed using a PDP 11/03L computer incorporated into the XSAM 800 spectrometer. A nine-point least-squares quadratic procedure was employed to smooth the spectra. The shapes were fitted assuming a linear background and Gaussian singlet lines. The constraints introduced to ensure that the results make physical sense are summarized in Table 2. They are derived from the analysis of the oxidized samples (line width, except for Mo(0), B.E. difference between doublet components), from the Scofield ionization cross sections (*35*) (intensity ratio between doublet components),

TABLE 2

Constraints Employed in the Analysis of Mo 3*d* Signal Shapes of Reduced MoO_3/Al_2O_3 Catalysts

FWHM (eV)	$I(Mo\ 3d_{3/2})/I(Mo\ 3d_{5/2})$	B.E. differences (eV)			
		Mo $3d_{3/2}$ − Mo $3d_{5/2}$	Mo(VI) −Mo(V)	Mo(VI) −$Mo(IV)_{is}$	Mo(VI) −"Mo(II)"
2.80[a] ±0.05	0.68 ±0.02	3.10 ±0.05	0.8 ±0.1	1.6 ±0.1	3.2 ±0.1

[a] Except for Mo(0).

and from the assumption of a linear relation between Mo binding energies and oxidation states (*33*). All states except Mo(0) have been treated as a set of doublets separated by defined B.E. differences. In the course of the analysis, the position of this set on the B.E. scale, the intensity contribution of the individual components, and the position, width, and intensity contribution of the Mo(0) doublet have been fitted.

As outlined in (*33*), the spectra usually do not allow an unambiguous analysis of Mo(V) and Mo(IV), but a range of possible concentrations for these states may be derived from the consideration of limiting cases (Mo(V) = 0 and Mo(V) = maximum, see Fig. 4, insert). Lines with a binding energy typical of Mo(II) can originate from Mo(II) or from paired double-bonded Mo(IV) ions as discussed for MoO_2 (*32*). The line with this B.E. is, therefore, denoted as "Mo(II)," the line with a B.E. typical of Mo(IV) is ascribed to isolated Mo(IV), $Mo(IV)_{is}$.

In some of the spectra shown in Fig. 4, a small "ghost peak" is visible at ≈225 eV (Figs. 4i, 4l, 4n). This peak is an artifact arising from incomplete shielding of the sample holder by the sample. It is a Mo(0) $3d_{5/2}$ component originating from a Mo contamination in the sample holder and shifted from the expected B.E. due to the difference in charging between sample and sample holder. In the analysis of the spectra (signal shape analysis as well as intensity calculation) the corresponding Mo(0) doublet has been removed.

3. EPR measurements. Samples for EPR measurements were prepared in a quartz flow reactor with a side arm connected with a sealable EPR sample tube. The method was described in some detail in (*23*). The EPR spectra were recorded at room temperature with an ERS 220 spectrometer (Scientific Equipment Center, former G.D.R. Academy of Sciences) operating in the X band and equipped with a 100-kHz field modulation.

4. Determination of the reduction degree (e/Mo). The reduction degree after treatments corresponding to those applied in the XPS experiments was determined by pulse reoxidation at 823 K (carrier gas neon). The reoxidation was completed by cycling a known amount of an O_2/Ne mixture over the catalyst and measuring the oxygen consumed after an appropriate time interval (usually less than 0.1 *e*/Mo in 30 min). A different method for the assessment of reduction degrees involves the determination of hydrogen consumption from a known amount of a H_2/Ne mixture cycled over the catalyst. When these methods were compared employing sample Mo7, which was reduced to 1.0–1.5 *e*/Mo, the reoxidation method showed a constant deviation of −0.2 to −0.3 *e*/Mo. A possible origin of this deviation is the reversible hydrogen, which is included in the hydrogen consumption measurement, but also a partial reoxidation of the reduced surface in flowing inert gas. A reoxidation of reduced Mo surface species in inert atmosphere will be shown to proceed to a considerable extent at 973 K (vide infra). Some reoxidation may have occurred in a ≈30-min period of Ne flow between reduction and reoxidation, which was necessary for the determination of water evolved.

The reduction degrees accessible with MoO_3/Al_2O_3 catalysts at 823 K were also determined by TPR. Samples of equal size were reduced in two parallel runs in 7 vol% H_2 in Ar. The first run, with an end temperature of 1170 K, maintained until the base line returned to zero, was assumed to correspond to *e*/Mo = 6. The other one, with an end temperature of 823 K, maintained for 2 h in the H_2/Ar flow and for 1 h in Ar, was compared with the previous one to obtain the reduction degree.

RESULTS

1. Oxidized state and thermal treatment in inert gas. In Figs. 1a–1d, typical Mo 3*d* signal shapes obtained from oxidized samples of catalysts with different MoO_3 content are shown. In Fig. 2, the Mo 3*d*/Al 2*s*

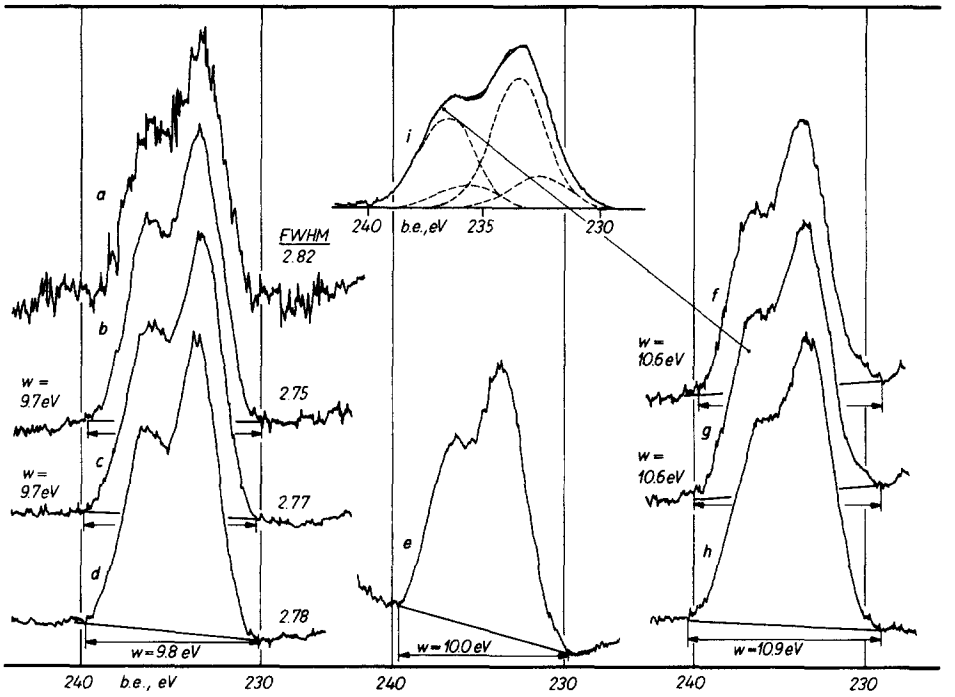

FIG. 1. Mo 3*d* spectra of calcined MoO_3/Al_2O_3 catalysts after different pretreatments. (a) Mo1, initial, (b) Mo4, initial, (c) Mo7, initial, (d) Mo13, initial, (e) Mo13, after Ar, 823 K, 1 h, (f) Mo4, after Ar, 973 K, 1 h, (g) Mo7, after Ar, 973 K, 1 h, (h) Mo 13, after Ar, 973 K, 1 h, (i) signal shape analysis of spectrum (g) with Gaussian lines, FWHM 2.80 eV. The FWHM specified in (a)–(d) were obtained by signal shape analysis.

intensity ratios are plotted versus the bulk atomic ratios and compared with the intensity ratios predicted for monolayer coverage by the stacking sheet model of Kerkhof and Moulijn ((*36*), for parameters see legend). An analogous comparison has been made for the WO_3/Al_2O_3 system with data from (*21*), where the Al 2*p* line had been used for this purpose.

It can be seen that the shape of the Mo 3*d* signal is nearly independent of the Mo content of the samples. Obviously, the considerable changes in the coordination of the Mo(VI) species in the range of MoO_3 contents covered, which should be expected on the basis of the literature (e.g., *29, 37, 38*), are not reflected in the Mo 3*d* signal shape. The FWHM of the support lines (Al 2*s*, O 1*s*) do not depend on the MoO_3 content either. The B.E. of Mo $3d_{5/2}$ is 233.1–233.2 eV, which is lower by ≈0.5 eV than the B.E. of MoO_3 measured with the same instrument (*33*).

At low Mo loading (≤0.7 Mo atoms/nm^2) the Mo 3*d*/Al 2*s* intensity ratios are proportional to the Mo/Al bulk ratio and coincide with the predictions made for monolayer dispersion on the basis of the Kerkhof–Moulijn model (Fig. 2). Deviations from the monolayer prediction occur already below the theoretical monolayer coverage, as reported earlier in (*39*). The conclusion that the molybdenum is not dispersed in an ideal monolayer at higher MoO_3 content is supported by the observation that the relative Mo intensity is increased by a thermal treatment in Ar at 973 K (Fig. 2, open symbols). The data on WO_3/Al_2O_3 catalysts (*21*) obey the monolayer prediction up to 3 W atoms/nm^2; for this prediction, the parame-

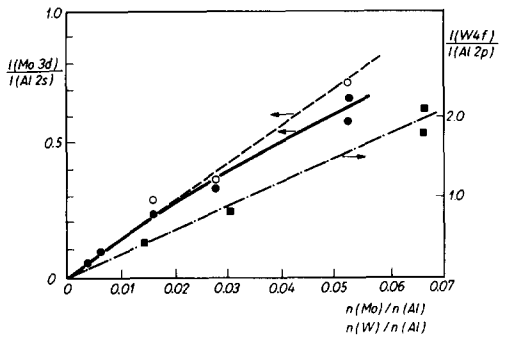

FIG. 2. Me/Al intensity ratios of MoO_3/Al_2O_3, in comparison with WO_3/Al_2O_3. MoO_3/Al_2O_3: (—●—) oxidized samples, (○) oxidized samples after Ar, 973 K, 1 h. WO_3/Al_2O_3: (■) oxidized samples, data from (*21*). Predictions for monolayer coverage according to (*36*): (———) MoO_3/Al_2O_3 parameters used: photoelectron cross sections, Mo 3*d*-9.74, Al 2*s*-0.68; mean free path lengths, $\lambda_{Mo\ 3d}$-1.40 nm, $\lambda_{Al\ 2s}$-1.52 nm, calculated according to (*36*) from λ (1400 eV) = 1.80 nm as suggested there; detector efficiency $D \sim E_{kin}^{1.5}$, support surface area-260 $m^2\ g^{-1}$; support density-3500 kg m^{-3}, (— · — · —) WO_3/Al_2O_3 parameters used: photoelectron cross sections, (W 4*f* + W 5$p_{3/2}$) – 10.6, Al 2*p* – 0.54; mean free path lengths $\lambda_{W\ 4f}$ – 2.63, $\lambda_{Al\ 2p}$ – 1.8 (*36*); remaining parameters as above.

ters recommended in (*36*) were employed with the detector transmission function of the instrument used in (*21*) (ES 200 B (*40*)).

The spectra shown in Figs. 1e–1h demonstrate the effect that a treatment of the initial samples in Ar at elevated temperature (823 K, 973 K) exerts on the Mo 3*d* signals. The shapes of these signals are clearly modified and significantly broadened at the base line. This suggests that a reduction has taken place, the product of which is most likely Mo(V).

Unfortunately, the evaluation of the Mo(V) content from these spectra is somewhat arbitrary at present, in particular for the samples treated at 973 K. Mo 3*d* spectra of samples obtained after calcination in air at this temperature did not indicate unambiguously which line width must be employed in the analysis of the signal shapes recorded with Ar-treated samples. At low MoO_3 content the signals were slightly broadened after calcination in air while their B.E. remained unchanged and their shapes corresponded to those of the initial state as shown in Figs. 1a–1d (Mo7: B.E. ($3d_{5/2}$) = 233.0 eV, FWHM = 2.88 eV after 1 h Ar, 973 K). At high MoO_3 content the FWHM decreased considerably (Mo13: B.E. ($3d_{5/2}$) = 233.2 eV, FWHM = 2.46 eV after 1 h Ar, 973 K). These phenomena, which suggest that different processes occur during thermal treatment in air and in inert gas, will be subject to future research. With a FWHM of 2.80 eV, i.e., slightly higher than in the initial samples, Mo(V) contributions of 17.5, 19, and 23% of total Mo were obtained for Mo4, Mo7, and Mo13, respectively, after treatment in Ar at 973 K. A Mo(V) contribution of 11% was derived for Mo13 treated at 823 K (i.e., the calcination temperature of the initial samples; cf. Experimental section). Despite the limited accuracy of these results, the tendency of a slight increase (or, at least, the absence of a decrease) of the reduction degree with increasing MoO_3 content at 973 K is, certainly, significant. It parallels the well-known properties of MoO_3/Al_2O_3 catalysts in the reduction by H_2 (*27, 29, 41*).

On a qualitative level, the formation of Mo(V) during thermal treatment of MoO_3/Al_2O_3 catalysts in flowing inert gas is supported by preliminary EPR investigations. Figure 3 shows the EPR spectra of samples treated in Ar at 973 K. Apart from the O_2^-

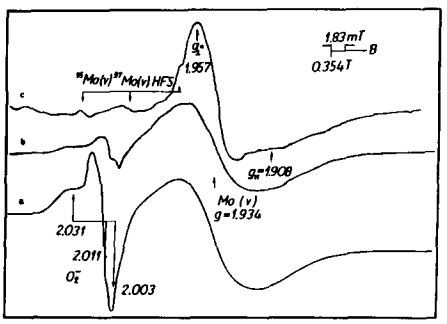

FIG. 3. EPR spectra of MoO_3/Al_2O_3 catalysts after 1-h Ar treatment at 973 K. (a) Mo4; (b) Mo7; (c) Mo13.

signal present, which is probably due to an experimental shortcoming (incomplete replacement of air in the sample tube prior to the run, O_2^- may be formed by reaction of O_2 with Mo(V) at room temperature (*42*)), the *g* values and the Mo hyperfine structure found with Mo13 prove the formation of Mo(V) (cf. *42, 43*) during the thermal treatment in Ar. In the oxidized state, these samples did not exhibit EPR signals.

Again, serious problems were encountered in the quantitative evaluation of the Mo(V) content. An attempt to assess the spin intensities of the Mo signals (reference ultramarine) supplied Mo(V) contents of <1% of the total Mo. Inaccuracies inherent in the procedure employed to separate the O_2^- and the Mo signals and, possibly, in the choice of the ultramarine standard, are of negligible order of magnitude compared with the difference in the XPS results. The presence of the O_2^- signal does not prove a contamination of the gas flows in the sample preparation, as the Mo(V) intensity was not higher in the absence of O_2^- (Mo13). In view of these problems (cf. also Discussion section) it was not attempted to establish the temperature of beginning Mo(V) formation in this preliminary stage of the EPR investigation.

2. Reduction of MoO_3/Al_2O_3 catalysts in H_2. Figure 4 shows typical Mo 3d spectra of MoO_3/Al_2O_3 catalysts after reduction at different temperatures (Figs. 4d, 4e, 4f, 4g, 4m, 4n, 4o, 4p). The influence of a subsequent Ar treatment at 973 K and a readmission of H_2 at 823 K, which induce dramatic changes of the metathesis activity (cf. part II of this work (*25*)), has also been studied (Figs. 4h, 4i, 4k, 4l). The spectra of the oxidized samples have been included for comparison (Figs. 4a–4c). An example of how to fit the Mo 3*d* signal shapes according to the principles described in the Experimental section is presented in the insert of the figure. The binding energies obtained in the analysis of the spectra are summarized in Table 3. It should be kept in mind, however, that in the course of the fitting procedure only the B.E. of Mo(VI) and of Mo(0) are determined independently (see Experimental section).

TABLE 3

Mo $3d_{5/2}$ Binding Energies Determined by Mathematical Analysis of Mo 3*d* Signal Shapes of Reduced MoO_3/Al_2O_3 Catalysts

Mo state	B.E. (eV)	s^a	n^b
VI	233.15[c]	0.15	45
V[d]	232.30	0.15	36
IV_{is}[d]	231.50	0.15	40
II[d]	229.90	0.15	36
0	228.80[c]	0.25	6

[a] Standard deviation: $s = \Sigma \{(\text{B.E.} - \overline{\text{B.E.}})^2/(n-1)\}^{1/2}$.

[b] Number of spectra included.

[c] For comparison: Mo(VI) in MoO_3, 233.6 eV (FWHM = 1.80 eV). Mo(0) obtained by reduction of MoO_3, 229.3 eV (FWHM = 1.45 eV).

[d] B.E. value predetermined by constraints; see Table 2.

Figure 5 presents the distribution of Mo states obtained above for different reduction temperatures. It can be seen that the catalysts are already reduced to a considerable extent at 673 K. On the surface of Mo13, even the "Mo(II)" state is present at this reduction temperature. Metallic molybdenum can be observed already at a reduction temperature of 900 K. While its contribution must be extracted from the spectra by signal shape analysis in the case of Mo4 and Mo7, it is quite obvious for Mo13 at this temperature and for Mo4 and Mo7 at 973 K (cf. Fig. 4). In Fig. 6, the progress of the reduction with time-on-stream is demonstrated for a reduction temperature of 823 K. Figures 5 and 6 reflect the well-known tendency of increasing reducibility of alumina-supported MoO_3 with increasing MoO_3 content (*27, 29, 47*).

The single points in the diagrams of Fig. 6 indicate that a thermal treatment in inert gas to remove adsorbed hydrogen from the surface leads to a partial reoxidation of the catalyst. This behavior, which is clearly reflected in the Mo 3*d* signal shapes (compare

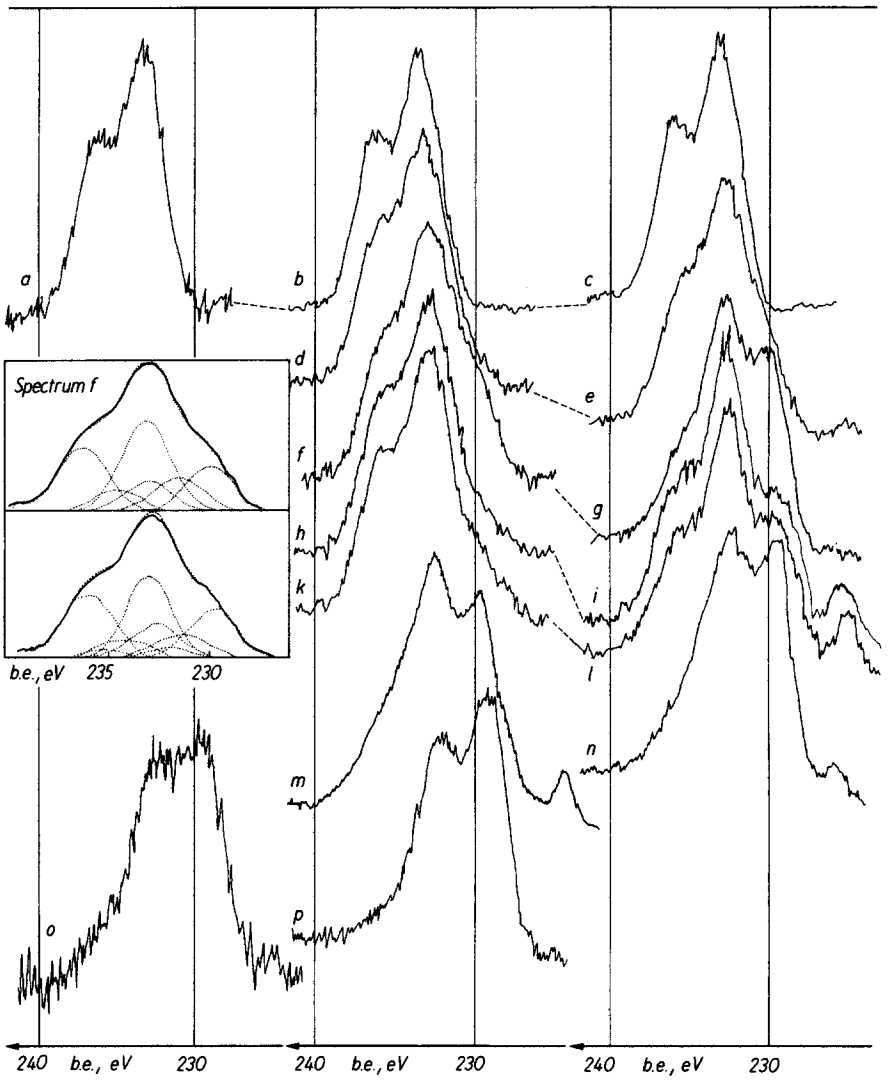

FIG. 4. Mo 3*d* XPS spectra of reduced MoO_3/Al_2O_3 catalysts. Initial samples: (a) Mo2, (b) Mo7, (c) Mo13. 2h H_2, 673 K: (d) Mo7, (e) Mo13. 30 min H_2, 823 K: (f) Mo7, (g) Mo13. 30 min H_2, 823 K + 2 h Ar, 973 K: (h) Mo7, (i) Mo13. 30 min H_2, 823 K + 2 h Ar, 973 K + 2 min H_2, 823 K: (k) Mo7, (l) Mo13. 2 h H_2, 900 K: (m) Mo7, (n) Mo13. 2 h H_2, 973 K: (o) Mo2, (p) Mo7. An example for the fitting of the spectra according to (*33*) is given in the insert. The spectrum used is spectrum f.

Figs. 4f and 4h with 4g and 4i), is documented in more detail in Table 4. A drastic decrease in the "Mo(II)" state and an increase in Mo(VI) is obvious for all samples, while $Mo(IV)_{is}$ (and possibly Mo(V)) is affected only at high MoO_3 content. A subsequent hydrogen treatment at 823 K for 2 min slightly moves the distribution of the Mo states back toward the pattern observed after the reduction. The differences are, however, near the detection limits inherent in the complex signal shape analysis procedure employed. A slight increase of "Mo(II)" at the expense of $Mo(IV)_{is}$ appears likely while the Mo(VI) state clearly remains on the high level obtained after the desorption procedure.

Table 4 also contains data showing the

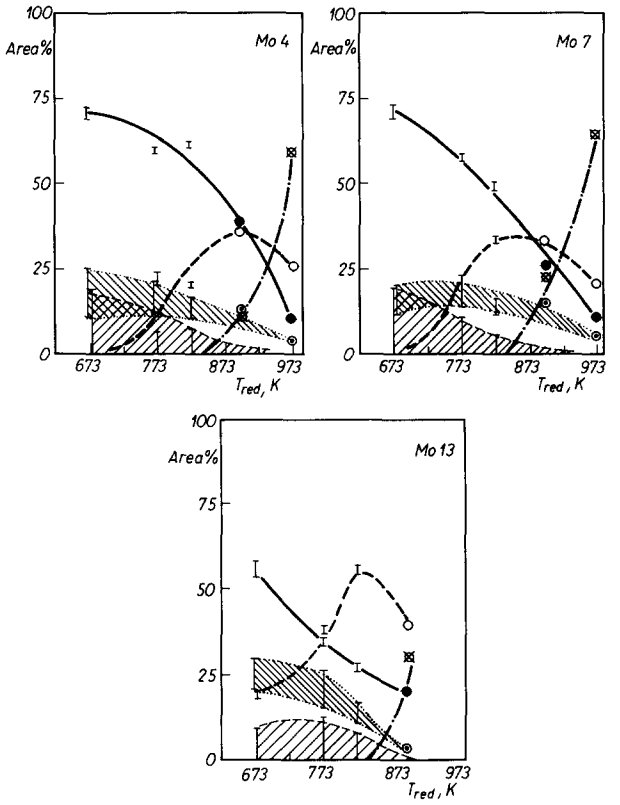

FIG. 5. Reduction of MoO_3/Al_2O_3 catalysts in H_2. Distribution of Mo states at different reduction temperatures. Reduction time, 2 h. ——●—— Mo(VI), possible range of Mo(V), possible range of $Mo(IV)_{is}$, – – –○– – "Mo(II)," —·—⊠—· Mo(0).

influence of oxygen traces in the carrier gas on the reduction extent. It can be seen that the preliminary runs performed with less carefully purified hydrogen resulted in significantly lower reduction degrees.

Figure 7 summarizes the results of intensity measurements with reduced MoO_3/Al_2O_3 catalysts, the Mo components of which exhibit the distribution of oxidation states reported in Figs. 5 and 6. While any trend is obscured by considerable scatter in the case of Mo13, a tendency to decrease relative Mo intensity with increase of reduction temperature is quite obvious with Mo4 and Mo7. This decrease is already detected at a reduction temperature of 823 K, i.e., before metallic Mo is present. An Ar treatment at 973 K for 2 h after the reduction leads to an increase in the Mo/Al intensity ratio, which corresponds to the observations made with the oxidized samples. Repeated short contact of the surfaces with H_2 at 823 K does not induce further significant changes in intensity.

The reduction degrees e/Mo of Mo7 and Mo13 reduced at 823 K have been derived from the analysis of the XPS spectra displayed in Fig. 6. In Fig. 8 they are compared with the results of the analysis by reoxidation and by TPR. The reduction degree estimated from the XPS spectra is calculated twice—with Mo(II) being assumed to be paired Mo(IV) or Mo(II). The scatter due to the uncertainty of Mo(V), (Mo(V) =

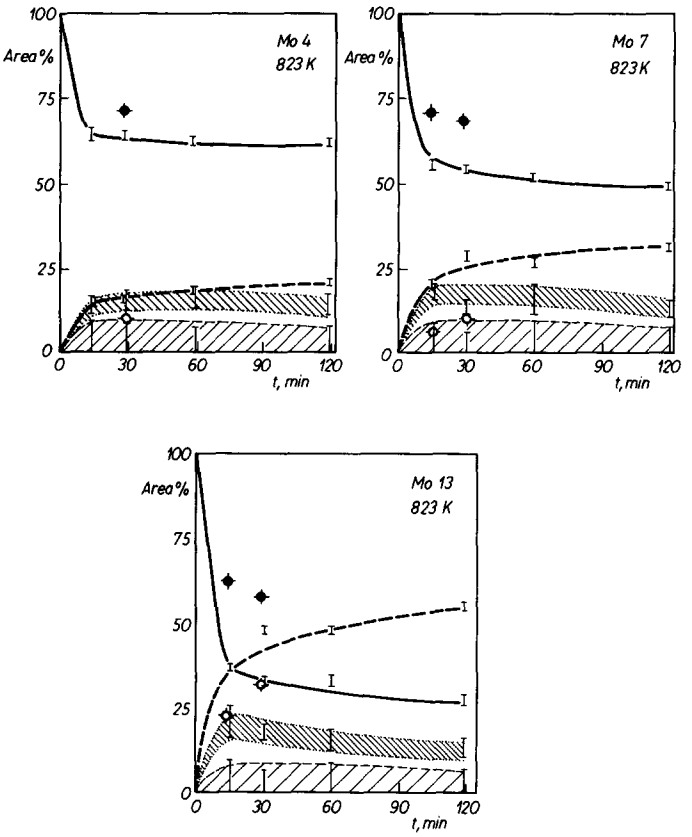

FIG. 6. Reduction of MoO_3/Al_2O_3 catalysts in H_2 at 823 K. Distribution of Mo states at different reduction times. For meaning of symbols see Fig. 5 legend. (-◆-) Mo(VI) after additional 2 h Ar 973 K, (-◇-) "Mo(II)" after additional 2 h Ar 973 K.

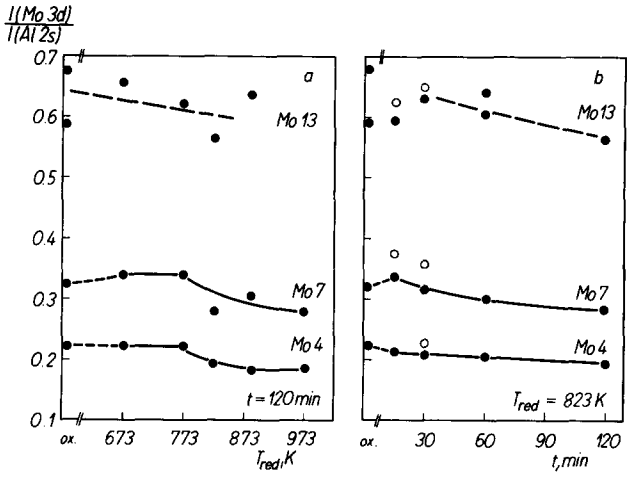

FIG. 7. Mo 3*d*/Al 2*s* intensity ratios of MoO_3/Al_2O_3 catalysts reduced in hydrogen. (a) Reduction time 2 h, (b) reduction temperature 823 K. Solid symbols, reduction in hydrogen; open symbols, with subsequent 2 h Ar, 973 K treatment.

TABLE 4

Distribution of Mo States on the Surface of MoO_3/Al_2O_3 Catalysts after Reduction in H_2 and after Subsequent Thermal Treatment in Ar

Catalyst	Pretreatment agent T_{act} (K); time (min)	Mo(VI)	Mo(V) min–max	$Mo(IV)_{is}$ max–min	"Mo(II)"	Mo(0)
Mo2	H_2 973; 120[a]	12	0[b]	11[b]	27	50
Mo4	H_2 823; 30	64	0–9	18–13	15	0
	H_2 823; 30 + Ar 973; 120	72	0–9	18–10	9	0
	H_2 823; 30 + Ar 973; 120 + H_2, 823; 2	71	0–7	14–12	12	0
	H_2 823; 120	62	0[b]	18[b]	20	0
	H_2 823;120[c]	71	0[b]	20[b]	9	0
	H_2 973; 120	12	0[b]	5[b]	25	58
	H_2 973; 120[c]	25	0[b]	43[b]	23	19
Mo7	H_2 823; 15	56.5	0–9	21–15.5	21	0
	H_2 823; 15 + Ar 973; 120	74	0–7	16–12	8	0
	H_2 823; 30	54.5	0–6	16.5–10.5	29	0
	H_2 823; 30 + Ar 973; 120	70	0–8	18–10	11.5	0
	H_2 823; 30 + Ar 973; 120 + H_2 823; 2	68.5	0–7	15–9.5	16	0
Mo13	H_2 823; 15	37.5	0–9	25–16	37	0
	H_2 823; 15 + Ar 973; 120	64	0–5	12–9	23	0
	H_2 823; 30	33	0–6	19–15	47	0
	H_2 823; 30 + Ar 973; 120	58	0[b]	8[b]	34	0
	H_2 823; 30 + Ar 973; 120 + H_2 823; 2	55	0[b]	5[b]	40	0
	H_2 823; 120	28.5	0[b]	16.5[b]	55	0
	H_2 823; 120[c]	29	0[b]	38[b]	33	0

Note. Amounts of Mo states given in area % of the total Mo 3*d* signal. Minor deviations from the sum of 100% may occur as values averaged from the analyses of the limiting cases (with and without Mo(V)—see Experimental) are given for all states.

[a] Spectrum shown in Fig. 4o.

[b] Only one limiting case (minimum of Mo(V) and maximum of $Mo(IV)_{is}$) analyzed.

[c] Preliminary run (oxygen traces in carrier gas, cf. Experimental).

0, or $Mo(V) = Mo(V)_{max}$) is not larger than the symbols used in the figure.

The values obtained from the reoxidation method are almost always higher than those derived from the XPS spectra with "Mo(II)" = $Mo(IV)_{paired}$. In the case of Mo13 they are close to the XPS data treated with "Mo(II)" = Mo(II). Notably, with both catalysts a significant increase of the reduction degree with reduction time is found in the reoxidation data and the XPS results when evaluated with "Mo(II)" = Mo(II), but not when treated with "Mo(II)" = $Mo(IV)_{paired}$. The TPR experi-

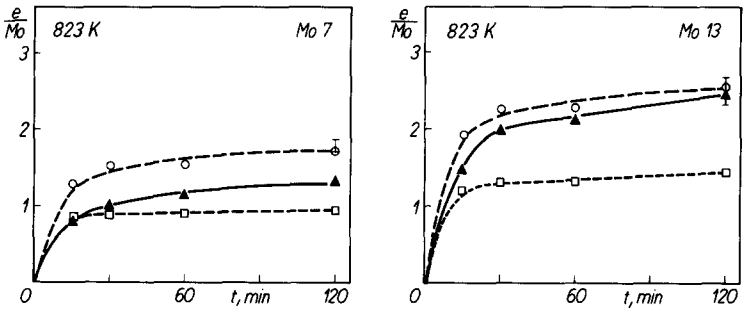

FIG. 8. Reduction degree of MoO_3/Al_2O_3 catalysts reduced in H_2, analyzed by different methods. (○) XPS, "Mo(II)" = Mo(II); (□) XPS, "Mo(II)" = paired Mo(IV); (▲) reoxidation method; (⌶) TPR (in 7 vol% H_2/Ar). For experimental details see text.

ments also supplied *e*/Mo values clearly above those expected with "Mo(II)" = $Mo(IV)_{paired}$. This observation is relevant despite some differences in the reduction regime between TPR and the XPS sample pretreatment (use of H_2/Ar mixture instead of pure H_2, longer effective reduction time, different sample forms and flow regimes, cf. Discussion): The approach "Mo(II)" = $Mo(IV)_{paired}$ yields rather rigid limits for the reduction degrees to be obtained with Mo7 and Mo13 at the reduction temperature employed. These are clearly exceeded in the TPR experiments.

DISCUSSION

1. Oxidized state and thermal treatment in inert gas. There is no doubt that the state of Mo in the initial samples is +6, as has often been reported (*27–31*), and the Mo $3d_{5/2}$ B.E. agrees well with most of the values given by other authors (*28–31*) provided that the same internal reference (e.g., Al 2*p* = 75.0) is employed. We would not draw any conclusion from a difference between the B.E. of unsupported MoO_3 (≃233.6 eV) and the supported catalysts (≃233.1–233.2 eV), which we have confirmed on a second instrument (ES 200B). Other authors report identical Mo(VI) B.E.s for MoO_3 and MoO_3/Al_2O_3 ((*31*) with C reference, (*29*) with Au reference) or even a higher B.E. for the supported catalyst ((*27*) with Au reference). Probably these discrepancies reflect referencing problems when samples of different conductivity (charging was ≃0.5 eV with MoO_3 and ≃4 eV with the alumina-supported samples) must be compared. A similar B.E. difference between supported and bulk material is found for Mo(0) (Table 4).

The Mo/Al intensity data displayed in Fig. 2 suggest the presence of bilayered or clustered molybdate structures already at MoO_3 contents below the theoretical monolayer coverage. This is what should be expected from the models of the MoO_3/Al_2O_3 surface widely accepted in the literature (*37, 41, 45*). Other authors found the relative Mo intensities to be proportional to the Mo/Al bulk ratio until the first (theoretical) monolayer is completed (*38, 46*). Actually, the impregnation method applied in our work may be suspected to favor clustering tendencies at high MoO_3 content (high pH of the impregnation solution possibly leading to precipitation of nonadsorbed molybdate onto the support). The high reduction degrees measured in our work (vide infra) might support this suspicion. The UV–VIS spectra of our catalysts did not exhibit signals attributable to MoO_3 entities ((*47*), cf. part II of this paper (*25*)) but structural data from more powerful methods are, unfortunately, not available at present. While this uncertainty in the structural properties of our catalysts does not affect the conclusions to be drawn in this paper, an investi-

gation of Mo catalysts of different origin by a combination of structural methods and the XPS technique applied in this work appears promising.

Both XPS (Figs. 1e–1h) and EPR (Fig. 3) prove that MoO_3/Al_2O_3 catalysts are partly reduced to Mo(V) by treatment in flowing inert gas at 973 K. In view of the probable presence of clustered molybdate structures weakly interacting with the support, this result is not surprising. Unsupported MoO_3 undergoes thermal reduction in inert gas to a large extent (*33*).

The results of the quantitative analysis of Mo(V) in the thermally treated samples by XPS and EPR diverged by orders of magnitudes. The Mo(V) quantities detected by EPR are so small that they would not be expected to cause any change in the XPS signal shapes. It is well known, however, that Mo(V) may escape detection by EPR if present in magnetically interacting pairs (*44*) and that this effect is most pronounced in systems with a highly clustered molybdate phase (e.g., MoO_3/SiO_2 compared to MoO_3/Al_2O_3 (*44, 48*)). Mo(V) quantities sufficient to significantly modify the XPS signal of the prevailing Mo(VI) state ($\geq$10% rel.) are likely to involve a considerable amount of Mo(V) pairs, the more so as they should be concentrated in the most reducible, clustered part of the supported Mo component. A procedure aimed at the decoupling of Mo(V) pairs, which involves a treatment with dry HCl, has been successfully applied to reduced MoO_3/Al_2O_3 and MoO_3/SiO_2 catalysts (*44, 48*). Probably, this approach has the potential to resolve the discrepancies described above. However, its application to our still highly oxidized samples does not appear to be straightforward because of the reducing properties of HCl (*23, 44*). While a precise analysis of the Mo(V) content in thermally treated MoO_3/Al_2O_3 requires further effort we believe that the assessment of the reduction degree by XPS (see Results section) properly reflects the order of magnitude of the Mo(V) contribution and its tendency with varying MoO_3 content.

2. Reduction of MoO_3/Al_2O_3 catalysts in H_2. The spectra obtained in this study and presented by typical examples in Fig. 4 qualitatively correspond to other spectra of reduced MoO_3/Al_2O_3 published in the literature (*26–31*). However, owing to our particular approach to the assignment of Mo states to Mo B.E. (*33*), the conclusions drawn by us differ considerably from those of other authors as discussed below.

Although our results confirm the existence of an initial period of rapid reduction in the temperature range 773–823 K, we have not found that all Mo(VI) is consumed in this initial phase yielding Mo(V) contributions as high as 70%, as suggested in (*29*). Instead, our analysis has shown that residual amounts of Mo(VI), depending on the total Mo content and on the reduction temperature, still remain after 2 h of reduction even at temperatures above 823 K. The presence of Mo(VI) can be detected most convincingly in the spectra obtained at a reduction temperature of 823 K, where the signal shapes define the position of "Mo(II)" quite well. Then, the high B.E. region of the signals can be fitted only with significant Mo(VI) contributions as the constraints summarized in Table 2 must be obeyed.

In the past, large discrepancies were noted in the analysis of Mo(V) in reduced supported Mo catalysts by EPR (*63, 49, 50*) and XPS (*27–29, 49, 50*). Even after an improvement of the EPR technique by a chemical decoupling of Mo(V) pairs ((*44, 48*), cf. previous section) typical results from XPS exceed those from EPR by half an order of magnitude. We believe that both methods can be reconciled on the basis of our reinterpretation of the Mo XPS spectra. In the framework of former approaches to the relation between Mo B.E. and oxidation state, Mo(V) would have to be assigned to those curves that now represent the upper limit of $Mo(IV)_{is}$ (Figs. 5, 6). At a reduction temperature of 823 K (Fig. 6), this corresponds to 2–2.5 times the values that, in our approach, represent the upper limit of Mo(V). Nevertheless, the analysis

of Mo(V) in Mo catalysts remains troublesome: XPS supplies only a range of possible Mo(V) contributions (or, in situations where the presence of Mo(IV) can be excluded, suffers from large uncertainties—see previous section), while EPR requires additional chemical treatment of the samples involving the risk of side reactions (reduction). An attempt to measure Mo(V) by XPS and EPR on identical samples has been left for future research.

The nature of the "Mo(II)" signal is another point that deserves closer inspection. According to the assignments made in (*33*) (cf. Experimental section) it could be due to either paired Mo(IV) ions, as in MoO_2, or to Mo(II). In the literature, both states have already been assumed to be present on reduced MoO_3/Al_2O_3. Thus, it has been pointed out that the reduction of surface molybdate structures by H_2 removes their bonding with the alumina surface and leads to a clustering of the reduced Mo phase (*45, 51*), which is also supported by our intensity data (Fig. 7). Moreover, the presence of microcrystalline MoO_2 (as an analog to the MoS_2 slabs formed in the sulfided state (*37*)) has been discussed (*45*). On the other hand, investigations of the reduction stoichiometry (*52*) and of the IR spectra of probe molecules (*53, 54*) indicated that Mo(II) could be formed during the reduction, probably at edge positions of the MoO_2-like phase (*45*). In previous XPS investigations, the presence of Mo(II) on these surfaces has never been considered.

A discrimination between the two possibilities (paired Mo(IV) or Mo(II)) may be expected from a comparison of the reduction degrees *e*/Mo derived from the XPS spectra with the results of independent volumetric *e*/Mo analyses. Unfortunately, we were not able to perform these independent analyses in our XPS sample pretreatment facility. This may give rise to some objections concerning the compatibility of our parallel experiments (possible differences in carrier gas purity; different sample forms and flow regimes: pressed powder samples passed by the flowing gas in XPS, 0.2 to 0.4-mm particles in a plug flow reactor in the parallel experiments). Moreover, slight deviations of the real distributions of Mo states from those reported on the basis of signal areas (Figs. 5, 6) may arise from the small decrease of the relative Mo intensity during reduction. We therefore do not stress the rather good agreement between the XPS reduction degrees obtained with "Mo(II)" = Mo(II) and the results of TPR and most of the reoxidation experiments, even if some of the remaining differences in the latter case can be ascribed to experimental problems (see Experimental section). The more convincing point is the observed increase of the reduction degree with increasing reduction time. Indeed, beyond a reduction time of 15 min, the effect of the hydrogen treatment mostly consists of the transformation of $Mo(IV)_{is}$ to "Mo(II)" (Fig. 6), which does not contribute to *e*/Mo when "Mo(II)" is paired Mo(IV). We conclude, therefore, that on the reduced MoO_3/Al_2O_3 surfaces investigated a considerable contribution to the "Mo(II)" signal is due to Mo(II) species present.

Recently, much attention has been paid to the preparation (*14, 55, 56*) and the properties (*57–59*) of alumina-supported metallic molybdenum. The first catalysts of this type were prepared starting from $Mo(CO)_6$ (*55, 56*). It has been shown that similar catalyst systems can also be obtained by severe reduction of impregnated MoO_3/Al_2O_3 (*55, 58–60*) and an XPS study of the surfaces obtained has been published (*30*).

In our investigation, the formation of metallic Mo has been observed at reduction temperatures well below those employed by most of the other authors. Thus, we find high Mo(0) contents already at 973 K, while Holl *et al.* (*30*) did not see Mo(0) when they reduced a catalyst of comparable Mo loading at 1023 K in a static regime. Redey *et al.* (*59*) identified Mo(0) after reduction at 1173 K (first indications at 1073 K) by its catalytic effect in the hydrogenation of ben-

zene, but this method may not be suited to detect Mo(0) interacting with residual Mo ions. Reduction degrees higher than those reported in the literature can also be stated at temperatures below the range of Mo(0) formation (e.g., 773 and 823 K, by comparison with spectra published in (*27, 29, 30*) without relying on signal shape analysis).

As mentioned earlier these differences might be ascribed to a somewhat lower Mo dispersion in our samples compared to those used by other authors. However, in view of our experience with oxygen-contaminated gases ("preliminary runs," see Table 4) and of similar differences between our results and the literature in the thermal degradation of unsupported MoO_3 in inert gas (*33*), we believe that an influence of the partial pressure of oxygen (or water) on the reduction process, probably on its thermodynamics as discussed in (*61*), may contribute to these discrepancies. Indeed, in a study where a rigorous purification of the applied gases was well documented (*60*), an average reduction degree *e*/Mo of 4.10 was obtained in the reduction of a catalyst with 2.3 Mo atoms/nm^2 ($\triangleq$Mo13), at 923 K. As one cannot expect the presence of only a single Mo state under these conditions (cf. Fig. 4m–4p), this result is a strong indication of the formation of some Mo(0) already at this temperature. From our XPS spectra, *e*/Mo = 3.6 is found for Mo13 after reduction at 900 K ("Mo(II)" = Mo(II); reoxidation method *e*/Mo = 4.0). The data of Redey *et al.* (*59*) for a catalyst with 2.7 Mo atoms/nm^2 may be interpolated to yield *e*/Mo of 3.0 and 3.35 for 900 and 923 K, respectively, which are considerably lower than those given in (*60*) or found by us.

Our material does not supply evidence for the presence of Mo(III) or Mo(I) in reduced MoO_3/Al_2O_3 catalysts. No prominent peak or shoulder has been observed in the B.E. region, where these states should be expected from the linear correlation between Mo oxidation states and binding energies employed in this study. It is impossible, of course, to exclude any state by the analysis of XPS spectra composed of several superimposed lines. To the best of our knowledge, there is no evidence from other methods proving the presence of these states on the surface of reduced unsulfided MoO_3/Al_2O_3 catalysts. We have, therefore, not considered them in our discussion.

It should be noted that our approach to the interpretation of Mo 3*d* XPS spectra of Mo catalysts is at variance with the methods used in two recent publications (*62, 63*). In these papers, Mo oxidation states below +4 were reported for $Mo(CO)_6/Al_2O_3$ (*62*) and reduced MoO_3/TiO_2 (*63*), among them +3 (*63*). In the first case, differences to the oxide systems considered in the present paper may arise from the CO ligands originally present. On the other hand, the divergence between us and (*63*) is not easily explained at the moment. In both cases, the conclusions are based on a combination of signal shape analyses with determinations of the average reduction degree, however, with a gravimetric technique employed in (*63*). Future research will have to resolve the contradiction. In this respect we believe that the successful application of our XPS results in the analysis of the metathesis site precursors of MoO_3/Al_2O_3 catalysts (part II of this paper (*25*)) yielding assignments compatible with the earlier literature and with our own work on WO_3/Al_2O_3 catalysts (*22*) lends further support to our approach.

3. Influence of high-temperature Ar treatments on the reduced surface. Figures 4 and 6 as well as Table 4 show that the reduction degree of a reduced MoO_3/Al_2O_3 catalyst decreases when the surface is subjected to thermal treatment in inert gas at 973 K. The effect is most clearly reflected in the loss of "Mo(II)" (probably Mo(II)) and the increase of Mo(VI), which, of course, does not mean that these are the only states affected by reoxidation. The thermal treatment is accompanied by a redispersion process (Fig. 7), which parallels trends that have been observed with thermally treated oxidized samples (Fig. 2).

In view of the rigorous purification of the

gases used (see Experimental section) we do not expect that the surface was reoxidized by oxygen traces in the carrier gas Ar. In the literature it has been suggested that Mo(II) is reoxidized to Mo(IV) when the hydrogen adsorbed is pumped off at the temperature of reduction (*64*). It is possible that this process may also occur under the conditions applied by us, but it is not the only reaction proceeding. Recently, the reoxidation of reduced MoO_3/Al_2O_3 surfaces by thermal treatments has been proved by measuring average reduction degrees, and surface OH groups have been suggested to be the oxidizing agent (*60*):

$$-OH^- + Mo^{(n-1)+} \rightleftarrows Mo^{n+} + -O^{2-} + \tfrac{1}{2} H_2. \quad (1)$$

We think that our results confirm this view. The tendency of redispersion during reoxidation becomes plausible as a reversal of the clustering tendency during reduction ((*45, 51*), see also Fig. 7). The $-O^{2-}$ in Eq. (1) would then have to be regarded as an oxygen bridge between the support and the Mo^{n+}.

According to (*62*), readsorption of hydrogen (by short-time contact at 773–823 K) onto the surface, from which it had been stripped off previously, leads to reformation of the Mo(II) destroyed in the desorption process. In our study of the hydrogen readsorption (Fig. 4, Table 4) a slight increase of "Mo(II)," probably at the expense of $Mo(IV)_{is}$, has been observed. Mo(VI), however, which reacts rapidly when the oxidized surface is exposed to hydrogen under these conditions, remains nearly unchanged. Hence, although a slight tendency of reversal to the original distribution of Mo states can be stated, it is evident that the 2-min H_2 treatment at 823 K is far from being sufficient to restore the distribution of Mo states as it was after the reduction.

CONCLUSIONS

MoO_3/Al_2O_3 catalysts (2–13 wt% MoO_3) were investigated by XPS in the oxidized form, after thermal treatment in flowing Ar (973 K) and after reduction in H_2 (673–973K), which are conditions typically employed in the activation of these catalysts for the metathesis reaction. A new assignment of the Mo 3*d* XPS lines observed to the Mo oxidation states was applied. During the thermal treatment in flowing Ar part of the hexavalent Mo present in the initial samples underwent reduction to Mo(V), which was also identified by EPR. The reduction of alumina-supported Mo(VI) in H_2 was found to produce surfaces, on which Mo(VI), Mo(V), Mo(IV), Mo(II), and at reduction temperatures above 900 K, Mo(0) coexist. At reduction temperatures of about 800 K, the Mo(V) contribution did not exceed 10% of the total Mo content. The presence of the Mo(II) state was verified by parallel measurements of the average reduction degree by reoxidation and TPR techniques.

When reduced MoO_3/Al_2O_3 surfaces were subjected to thermal treatment in inert gas at 973 K, the Mo surface species were partly reoxidized. Readsorption of hydrogen by short-time contact at 823 K did not restore the previous distribution of Mo states.

ACKNOWLEDGMENTS

Thanks are owed to Drs. P. E. Nau, P. Kraak from Leuna-Werke, Leuna, and M. Henker from the Technical University in Merseburg for performing X-ray microprobe analysis, BET, and TPR measurements, respectively.

REFERENCES

1. Herisson, J. L., and Chauvin, Y., *Makromol. Chem.* **141,** 161 (1971).
2. Katz, Th. J., and Hersch, W. H., *Tetrahedron Lett.*, 585 (1977).
3. Howard, T. R., Lee, J. B., and Grubbs, R. H., *J. Am. Chem. Soc.* **102,** 6876 (1980).
4. Mol, J. C., and Moulijn, J. A., *in* "Advances in Catalysis" (D. D. Eley, H. Pines, and P. B. Weisz, Eds.), Vol. 24, p. 131. Academic Press, San Diego, 1975.
5. Iwasawa, Y., *in* "Advances in Catalysis" (D. D. Eley, H. Pines, and P. B. Weisz, Eds.) Vol. 35, p. 187. Academic Press, San Diego, 1987.
6. Engelhardt, J., Goldwasser, J., and Hall, W. K., *J. Catal.* **76,** 48 (1982).
7. Anpo, M., Kondo, M., Kubokawa, Y., Louis, C.,

and Che, M., *J. Chem. Soc. Faraday Trans.* 1 **84,** 2771 (1988).
8. Kazuta, M., and Tanaka, K.-I., *J. Catal.* **123,** 164 (1990).
9. Nakamura, R., and Echigoya, E., *Nippon Kagaku Kaisshi* **12,** 2276 (1972).
10. Giordano, N., Padovan, M., Vaghi, A., Bart, J. C. J., and Castellan, A., *J. Catal.* **38,** 1 (1975).
11. Engelhardt, J., *J. Mol. Catal.* **8,** 119 (1980).
12. Shelimov, B. N., Elev, I. V., and Kazansky, V. B., *J. Catal.* **98,** 70 (1986).
13. Elev, I. V., Shelimov, B. N., and Kazansky, V. B., *Kinet. Katal.* **28,** 409 (1987).
14. Brenner, A., and Burwell, R. L., Jr., *J. Catal.* **52,** 364 (1978); Brenner, A., Hucul, D. A., and Hardwick, S. J., *Inorg. Chem.* **18,** 1478 (1979).
15. Komatsu, T., Namba, S., and Yashima, T., *Acta Phys. Chem.* **31,** 251 (1985).
16. Goldwasser, J., Engelhardt, J., and Hall, W. K., *J. Catal.* **70,** 275 (1981).
17. Seyferth, K., and Taube, R., *J. Mol. Catal.* **28,** 53 (1985).
18. Schrock, R. R., Krouse, S. A., Knoll, K., Feldman, J., Murdzek, J., and Yang, D. C., *J. Mol. Catal.* **46,** 243 (1988).
19. Luckner, R. C., and Wills, G. B., *J. Catal.* **28,** 83 (1973); Thomas, R., Moulijn, J. A., de Beer, V. H. J., and Medema, J., *J. Mol. Catal.* **8,** 161 (1980).
20. Anpo, M., Tanahashi, I., and Kubokawa, Y., *J. Chem. Soc. Faraday Trans. 1* **78,** 2121 (1982).
21. Grünert, W., Shpiro, E. S., Feldhaus, R., Anders, K., Antoshin, G. V., and Minachev, Kh. M., *J. Catal.* **107,** 522 (1987).
22. Grünert, W., Feldhaus, R., Anders, K., Shpiro, E. S., and Minachev, Kh. M., *J. Catal.* **120,** 444 (1989).
23. Grünert, W., Mörke, W., Feldhaus, R., and Anders, K., *J. Catal.* **117,** 485 (1989).
24. Grünert, W., Feldhaus, R., and Anders, K., *React. Kinet. Catal. Lett.* **36,** 195 (1988).
25. Grünert, W., Stakheev, A. Yu., Feldhaus, R., Anders, K., Shpiro, E. S., and Minachev, Kh. M., *J. Catal.* **135,** 287 (1992).
26. Cimino, A., and de Angelis, B. A., *J. Catal.* **36,** 11 (1975).
27. Patterson, T. A., Carver, J. C., Leyden, D. E., and Hercules, D. M., *J. Phys. Chem.* **80,** 1700 (1976).
28. Slinkin, A. A., Antoshin, G. V., Loktev, M. T., Shpiro, E. S., Nikishenko, S. B., and Minachev, Kh. M., *Izv. Akad. Nauk SSSR, Ser. Khim.,* 2225 (1978).
29. Zingg, D. S., Makovsky, L. E., Tischer, R. E., Brown, F. R., and Hercules, D. M., *J. Phys. Chem.* **84,** 2898 (1980).
30. Holl, Y., Touroude, R., Maire, G., Muller, A., Engelhard, P. A., and Grosmangin, J., *J. Catal.* **104,** 202 (1987).
31. Okamoto, Y., Imanaka, T., and Teranishi, S., *J. Catal.* **65,** 448 (1980).
32. Haber, J., Marczewski, W., Stoch, J., and Ungier, L., *Ber. Bunsenges. Phys. Chem.* **79,** 970 (1975).
33. Grünert, W., Stakheev, A. Yu., Feldhaus, R., Anders, K., Shpiro, E. S., and Minachev, Kh. M., *J. Phys. Chem.* **95,** 1323 (1991).
34. Grünert, W., Feldhaus, R., Anders, K., Shpiro, E. S., Antoshin, G. V., and Minachev, Kh. M., *J. Electron Spectrosc. Relat. Phenom.* **40,** 187 (1986).
35. Scofield, J. H., *J. Electron Spectrosc. Relat. Phenom.* **8,** 129 (1976).
36. Kerkhof, F. P. J. M., and Moulijn, J. A., *J. Phys. Chem.* **83,** 1612 (1979).
37. Knözinger, H., *in* "Proceedings, 9th International Congress on Catalysis, Calgary, 1988" (M. J. Phillips and M. Ternan, Eds.), Chem. Institute of Canada, Ottawa, 1988.
38. Okamoto, Y., and Imanaka, T. *J. Phys. Chem.* **92,** 7102 (1988).
39. Rodrigo, L., Marcinkowska, K., Adnot, A., Roberge, P. C., Kaliaguine, S., Stencel, J. M., Makovsky, L. E., and Diehl, J. R., *J. Phys. Chem.* **90,** 2690 (1986).
40. Minachev, Kh. M., Antoshin, G. V., and Shpiro, E. S., "Photoelektronnaya spektroskopiya i eyo primeneniye v katalize," Photoelectron Spectroscopy and its Application in Catalysis. Nauka, Moscow, 1981.
41. Thomas, R., van Oers, E. M., de Beer, V. H. J., Medema, J., and Moulijn, J. A., *J. Catal.* **76,** 241 (1982).
42. Shvets, V. A., and Kazansky, V. B., *J. Catal.* **25,** 123 (1972).
43. Seshadri, K. S., and Petrakis, L., *J. Phys. Chem.* **74,** 4102 (1970); *J. Catal.* **30,** 95 (1973).
44. Abdo, S., Kazusaka, A., and Howe, R. F., *J. Phys. Chem.* **85,** 1380 (1981).
45. Hall, W. K., *in* "The Chemistry and Physics of Solid Surfaces" (R. Vanselow and R. F. Howe, Eds.), Vol. VI. Springer-Verlag, Berlin New York, 1986.
46. Dufresne, P., Payen, E., Grimblot, J., and Bonelle, J. P., *J. Phys. Chem.* **85,** 2344 (1981).
47. Grünert, W., and Henker, M., unpublished results.
48. Seyedmonir, S. R., and Howe, R. F., *J. Chem. Soc. Faraday Trans. 1* **80,** 87 (1984).
49. Ward, M. B., Lin, M., and Lunsford, J. H., *J. Catal.* **50,** 306 (1977).
50. Mendelovici, L., and Lunsford, J. H., *J. Catal.* **94,** 37 (1985).
51. Liu, H. C., and Weller, S. W., *J. Catal.* **66,** 65 (1980).
52. Valyon, J., and Hall, W. K., *J. Catal.* **92,** 155 (1985).
53. Peri, J. B., *J. Phys. Chem.* **86,** 1615 (1982).
54. Delgado, E., Fuentes, G. A., Hermann, C., Kunz-

mann, G., and Knözinger, H., *Bull. Soc. Chim. Belg.* **93,** 82 (1984).

55. Brenner, A., and Hucul, D. A., *in* "Proceedings, 3rd International Conference on the Chemistry and Uses of Molybdenum (H. F. Barry and P. C. H. Mitchell, Eds.), p. 174, Ann Arbor, MI, 1979.
56. Nakamura, R., Bowman, R. G., and Burwell, R. L. Jr., *J. Am. Chem Soc.* **103,** 673 (1981).
57. Nakamura, R., Pioch, D., Bowman, R. G., and Burwell, R. L., Jr., *J. Catal.* **93,** 388, 399 (1985); Bowman, R. G., and Burwell, R. L., Jr., *J. Catal.* **63,** 463 (1980); Bowman, R. G., and Burwell, R. L., Jr., *J. Catal.* **88,** 388 (1984).
58. Holl, Y., Garin, F., Maire, G., Muller, A., Engelhard, P. A., and Grosmangin, J., *J. Catal.* **104,** 211, 225 (1987); Holl, Y., Garin, F., and Maire, G., *J. Catal.* **113,** 569 (1988); Holl, Y., Garin, F., Maire, G., Borg, F., Engelhard, P. A., and Grosmangin, J., *Appl. Catal.* **46,** 57 (1989).
59. Redey, A., Goldwasser, J., and Hall, W. K., *J. Catal.* **113,** 82 (1988).
60. Chung, J.-S., Zhang, J. P., and Burwell, R. L., Jr., *J. Catal.* **116,** 506 (1989); Chung, J.-S., and Burwell, R. L., Jr., *J. Catal.* **116,** 519 (1989).
61. Kung, H. H., "Transition Metal Oxides: Surface Chemistry and Catalysis" (B. Delmon and J. T. Yates, Eds.), Studies in Surface Science and Catalysis, Vol. 45. Elsevier, Amsterdam Oxford New York/Tokyo, 1989.
62. Goldwasser, J., Fang, S. M., Houalla, M., and Hall, W. K., *J. Catal.* **115,** 34 (1989).
63. Quincy, R. B., Houalla, M., Proctor, A., and Hercules, D. M., *J. Phys. Chem.* **94,** 1520 (1990).
64. Engelhardt, J., Kallo, D., and Zsinka, I., *J. Catal.* **88,** 317 (1984).